Indonesian Journal of Electrical Engineering and Computer Science
Vol. 42, No. 2, May 2026, pp. 307~317
ISSN: 2502-4752, DOI: 10.11591/ijeecs.v42.i2.pp307-317

Modeling and control of a solar-powered cable-driven robot under power constraints

Kendouli Fairouz[1], Hemama Aboud[2], Khoudir Abed[1]
[1]Department of Transport Engineering, Electrical Engineering Laboratory of Constantine (LGEC), Constantine 1 University, Constantine, Algeria
[2]Department of Transport Engineering, Constantine 1 University, Constantine, Algeria

Article Info

Article history:

Received Dec 16, 2025
Revised Apr 15, 2026
Accepted May 26, 2026

Keywords:

Cable-driven robot
Fuzzy logic control
PID control
Solar-powered systems
Trajectory tracking

ABSTRACT

This paper investigates the control performance of a solar-powered cable-driven robot using MATLAB simulations, comparing a conventional proportional–integral–derivative (PID) controller with a hybrid fuzzy PD controller. The study adopts a simplified kinematic model to focus on control behavior under cable-induced nonlinearities and time-varying power availability due to solar energy, while neglecting full dynamic and cable tension effects. Both controllers were systematically tuned to ensure a fair comparison. Performance was evaluated in terms of speed and position tracking under fluctuating solar conditions. Simulation results show that the hybrid fuzzy PD controller provides superior performance, with lower RMS tracking errors, reduced overshoot, and faster settling times compared to the PID controller. These findings highlight the potential of energy-aware intelligent control strategies for improving the reliability and accuracy of solar-powered cable-driven robots operating under variable renewable energy conditions.

Corresponding Author:

Kendouli Fairouz
Department of Transport Engineering, Electrical Engineering Laboratory of Constantine (LGEC)
Constantine 1 University
Constantine, Algeria
Email: kendouli.fairouz@umc.edu.dz

1. INTRODUCTION

Cable-driven robots are increasingly employed in lightweight systems and large-workspace applications due to their high payload-to-weight ratio and structural flexibility. However, their control remains challenging because of nonlinear cable tension effects, kinematic coupling, and sensitivity to external disturbances [1], [2]. When such robots are powered by photovoltaic energy sources, control performance can further degrade as a result of time-varying power availability caused by solar irradiance fluctuations [3]. Classical proportional–integral–derivative (PID) controllers, despite their simplicity and widespread industrial use, often exhibit limited robustness when applied to nonlinear and uncertain systems such as cable-driven robots [4]. In contrast, fuzzy logic–based controllers have demonstrated improved robustness and tracking performance in robotic applications with nonlinear dynamics [5], [6]. Nevertheless, most existing studies assume a stable power supply and do not explicitly consider the impact of renewable energy variability on control performance.

To address this research gap, this paper investigates the control of a solar-powered cable-driven robot by comparing a conventional PID controller with a hybrid fuzzy PD controller augmented with a fuzzy integral action. A simplified kinematic model is adopted to enable efficient control-oriented analysis while focusing on the combined effects of cable-induced nonlinearities and fluctuating solar power [1], [7]. Numerical simulations

are conducted to quantitatively evaluate speed and position tracking performance using RMS error, overshoot, and settling time as key metrics. The main contribution of this work lies in the explicit and simultaneous consideration of cable-driven nonlinearities and solar-induced power constraints within a unified control performance evaluation framework, which remains scarcely, addressed in existing literature [2], [3], [6].

2. SYSTEM DESCRIPTION

2.1. Geometry of a parallel robot with 4 cables

Cleaning high-rise façades is hazardous due to limited worker safety on ropes or suspended platforms. To address this, modular and rope-driven robots have been developed for precise and autonomous façade cleaning [8]-[10]. Building on these designs, this work investigates a solar-powered cable-driven robot under power constraints, comparing PID and hybrid fuzzy PD controllers through numerical simulations, with performance evaluated in terms of tracking accuracy, overshoot, and settling time.

2.1.1. Geometric description of the robot

The robot studied consists of four parallel cables (Figure 1). The mechanical structure of this robot consists of:

- A fixed base in rectangular form (frame)
- A mobile platform, which carries the terminal organ
- The base and the mobile platform are linked by four cables
- Each cable is linked to the base by an actuator (motors)

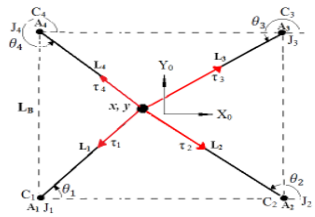

Figure 1. Parallel robot with 4 cables

- r: the radius of the pulley of each motor.
- m: the mass of the terminal organ.
- C: the viscous damping coefficients of each motor shaft.
- J: the inertias of the rotor and pulley of each motor.
- τ(i): the torques applied by the motors to the cables.
- Ai: the points of attachment of the cables to the motors.
- L_B: the length of the side of the rectangle limiting the work space.
- θi: the angle of rotation of the cables relative to the X axis.
- Li: cable lengths.

2.1.2. Geometric modeling

The direct geometric model provides the end-effector pose as a function of joint variables, while the inverse model gives joint variables for a desired pose. For serial robots, direct kinematics is straightforward, but inverse kinematics often requires numerical or analytical methods. In parallel robots, the inverse model is usually simpler, while the direct model may need numerical solutions [11]-[13]. Recent studies also address hybrid serial-parallel manipulators and advanced geometric methods to improve kinematic analysis for motion planning and control.

A. Inverse geometric model (IGM)

The purpose of this model is to determine the lengths of the cables "L_i" and the angles "θ_i" between the X axis and the cables as a function of the position {x, y}. The inverse geometric model can be expressed by the following relationships:

$$L_i = \sqrt{(x - A_{ix})^2 + \left(y - A_{iy}\right)^2}\,, i = 1,2,3,4 \quad (1)$$

$$\theta_i = arctang\left(\frac{y - A_{iy}}{x - A_{ix}}\right)\,, i = 1,2,3,4 \quad (2)$$

B. Direct geometric model (DGM)

The DGM expresses the position of the effector M(x, y) as a function of the lengths of the cables Li. For parallel manipulators, the direct geometric model is difficult to solve because of its closed structure (the expressions for the angles θi are mathematically linked with the lengths of the Li cables). The relationship between the position X=(x, y) and the generalized coordinates is non-linear [14].

This problem can be simplified by moving the reference frame $R(O,X_0,Y_0)$ to point A_1 which gives us new coordinates of the points $A_1=(0,0)^T$ and $A_2=(L_b,0)^T$.

Then the solution of the direct geometric model is the intersection of two circles, one with center A_1 and radius L_1, and the other with center A_2 and radius L_2. The position of the effector is expressed by the following relationships:

$$x = \frac{{L_b}^2+{L_1}^2-{L_2}^2}{2L_b} \tag{3}$$

$$y = \pm\sqrt{{L_1}^2 - x^2} \tag{4}$$

2.1.3. Kinematic modeling

In this part, we present the inverse and direct kinematic modeling of our parallel cable robot. This involves calculating the speed of the effector from MGD, and the speeds of the cables from the speed of the effector [15].

A. Inverse kinematic model

To calculate the inverse kinematic model, we consider the following ith (ième) vector:

$$x = A_{ix} + L_i\, cos\, cos\, (\theta_i)\; et\; y = A_{iy} + L_i\, sin\, sin\, (\theta_i) \tag{5}$$

$$\begin{pmatrix} x \\ y \end{pmatrix} = \begin{pmatrix} A_{ix} + L_i \cos(\theta_i) \\ A_{iy} + L_i \sin(\theta_i) \end{pmatrix} \tag{6}$$

the derivative of the position vector with respect to time is given by:

$$\begin{pmatrix} \dot{x} \\ \dot{y} \end{pmatrix} = \begin{pmatrix} \cos(\theta_i) & -L_i \sin(\theta_i) \\ \sin(\theta_i) & L_i \cos(\theta_i) \end{pmatrix} \begin{pmatrix} \dot{L}_\iota \\ \dot{\theta}_\iota \end{pmatrix} \; pour\; i = 1,2,3,4 \tag{7}$$

from this expression we deduce:

$$\begin{pmatrix} \dot{L}_\iota \\ \dot{\theta}_\iota \end{pmatrix} = \begin{pmatrix} \cos(\theta_i) & \sin(\theta_i) \\ \frac{-\sin(\theta_i)}{L_i} & \frac{\cos(\theta_i)}{L_i} \end{pmatrix} \begin{pmatrix} \dot{x} \\ \dot{y} \end{pmatrix} \; pour\; i = 1,2,3,4 \tag{8}$$

as we are interested in the length of the cables as a function of the position of the effector, we can extract the first line of (8) to obtain the inverse kinematic model of the robot.

$$\begin{pmatrix} \dot{L_1} \\ \dot{L_2} \\ \dot{L_3} \\ \dot{L_4} \end{pmatrix} = \begin{pmatrix} \cos(\theta_1) & \sin(\theta_1) \\ \cos(\theta_2) & \sin(\theta_2) \\ \cos(\theta_3) & \sin(\theta_3) \\ \cos(\theta_4) & \sin(\theta_4) \end{pmatrix} \begin{pmatrix} \dot{x} \\ \dot{y} \end{pmatrix} \tag{9}$$

B. Direct kinematic model

To obtain the direct kinematic model, we must invert equation (9) which gives us:

$$(\dot{X}) = M^{+}(\dot{L}) \tag{10}$$

with $M = \begin{pmatrix} \cos(\theta_1) & \sin(\theta_1) \\ \cos(\theta_2) & \sin(\theta_2) \\ \cos(\theta_3) & \sin(\theta_3) \\ \cos(\theta_4) & \sin(\theta_4) \end{pmatrix}$

$$(\dot{X}) = M^{+}(\dot{L})\; With\; M^{+} = (M^T M)^{-1} M^T \tag{11}$$

Or:

$\dot{L}$: speed vector of the 4 Cables

$(\dot{X}) = \begin{pmatrix} \dot{x} \\ \dot{y} \end{pmatrix}$, $\dot{X}$: the velocity vector of the effector.

M^{+}: the pseudo inverse of Moore-Penrose.

To facilitate the management and visualization of the robot's geometric model, a dedicated graphical user interface (GUI) was developed, as shown in Figure 2.

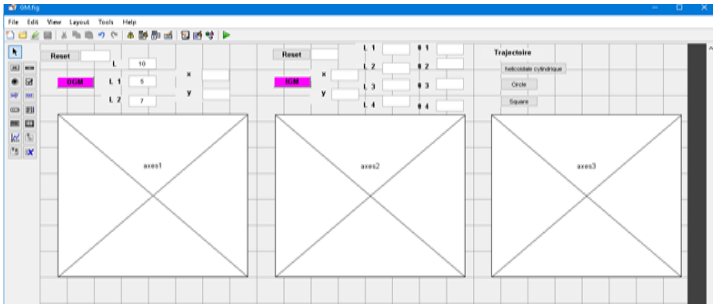

Figure 2. Graphical user interface for manages the geometric model

For the verification of both direct and inverse geometric models by taking two points $X_1(1, 3)$ and $X_2(2,-3)$, $L_b=10$.

- To check the IGM by taking the first position $X_1(1, 3)$, the cable lengths are: $L_1=10$cm, $L_2=8.94$, $L_3=4.47$, $L_4=6.32$.

We use the same lengths of the cables $L_1=10$cm, $L_2=8.94$, $L_3=4.47$, $L_4=6.32$ to check the DGM, we find the position of the effector is X (1, 3), as illustrated in Figure 3.

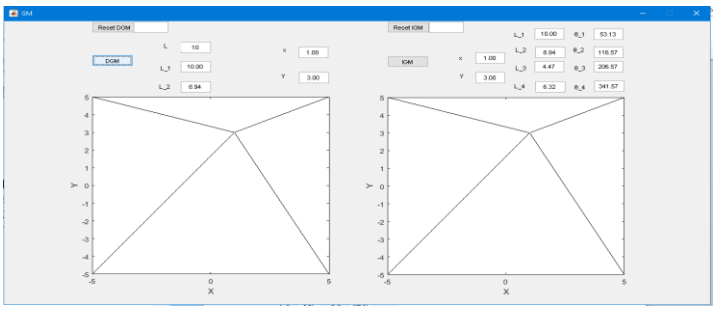

Figure 3. Graphical representation of IGM and DGM for x (1, 3)

- For the second position *X (2,-3)*, the cable lengths are: $L_1=7.28$cm, $L_2=3.61$, $L_3=8.54$, $L_4=10.63$.
- We use the same cable lengths for the same point X (2,-3), as shown in Figure 4.

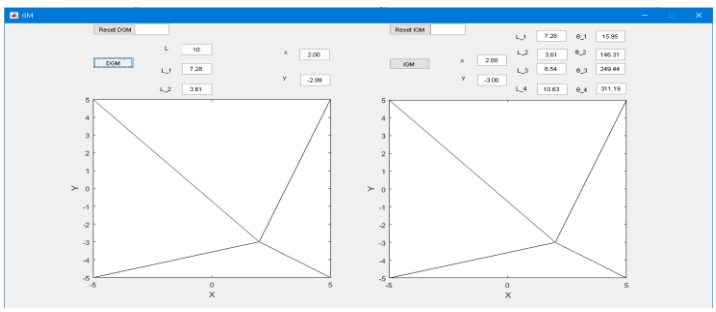

Figure 4. Graphical representation of IGM and MGD for *x (2,-3)*

2.2. Motor actuation system

Each cable of the proposed four-cable robot is driven by an independent DC motor, allowing precise platform positioning and stable motion under disturbances. DC motors are suitable for real-time feedback control [16], and coordinated motor control improves workspace performance and reduces vibrations [17]. Advanced control strategies, including PID and fuzzy controllers, further enhance tracking accuracy and robustness [18].

$$v = R * i + L * \frac{di}{dt} + ke * T = Kt * I \quad (13)$$

$$j * \frac{d\omega}{dt} = T - b * \omega - Tload \quad (14)$$

3. POWER CONSTRAINED MOTOR CONTROL UNDER VARIABLE SOLAR ENERGY

The *PV* array can be represented by a single diode equivalent circuit, which captures the nonlinear *I–V* characteristics of the *PV* modules. The *PV* current-voltage relation is given by [19]:

$$I_{PV} = I\_ph - I\_0 * (\exp((V\_PV + I\_PV * R\_s)/(n * V\_t)) - 1) - (V\_PV + I\_PV * R\_s) / R\_sh \quad (15)$$

where:

- *I_PV* and V_PV are the *PV* array output current and voltage.
- *I_ph* is the photo-generated current (proportional to irradiance).
- *I_0* is the diode saturation current.
- R_s and *R_sh* are the series and shunt resistances of the *PV* model.
- *n*V_t* represents the diode ideality factor times the thermal voltage.

The variability of solar energy is modeled by introducing a time-varying solar irradiance profile G(t), which directly affects the photo-generated current Iph. In the simulations, Iph is assumed to be proportional to the instantaneous irradiance, such that [20]:

$$I_{ph(t)} = I_{phref} * \frac{G(t)}{Gref} \quad (16)$$

Where Gref represents the nominal irradiance under standard test conditions. The irradiance profile G(t) is defined as a bounded time-varying signal to emulate realistic solar fluctuations caused by environmental conditions. The resulting variation in the available photovoltaic power is then used to constrain the motor input power within the control loop.

The instantaneous photovoltaic power P_PV(t) can then be calculated as:

$$P\_PV(t) = V\_PV.i\_ph(t) \quad (17)$$

Gref represents the nominal irradiance under standard test conditions.

V_PV(t) is the PV voltage at time t.

G(t) is a bounded time-varying signal that emulates realistic solar fluctuations caused by environmental conditions.

The resulting variation in the available photovoltaic power P_PV(t) is then used to constrain the motor input power within the control loop (Figure 5).

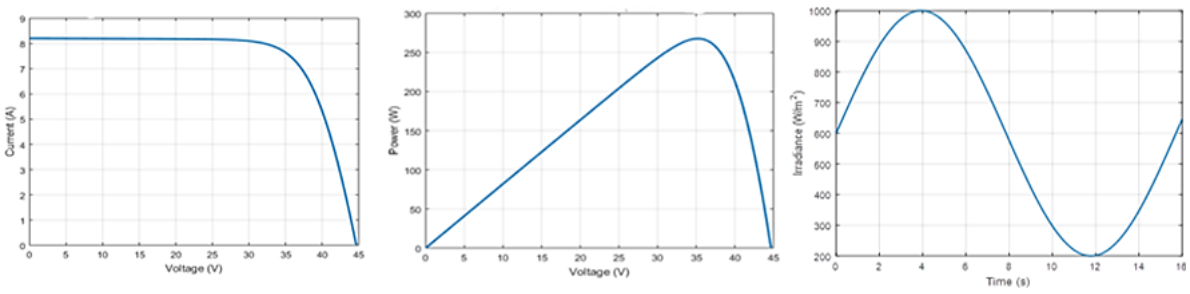

Figure 5. PV panel (voltage-current), (power-voltage), and irradiance over time

4. THEORETICAL BACKGROUND OF PID AND FUZZY CONTROLLERS

4.1. PID control: principle and equations

The PID controller is used to regulate motor speed by combining three complementary control actions:

- Proportional (P): generates an immediate control response proportional to the current tracking error.
- Integral (I): accumulates past errors to eliminate steady-state error.
- Derivative (D): predicts the future trend of the error, improving damping and reducing overshoot.

The PID control law is given by [21]:

$$u(t) = Kp \cdot e(t) + Ki \cdot \int e(\tau)\, d\tau + Kd \cdot (de(t)/dt) \quad (18)$$

where e(t) represents the speed tracking error, and Kp, Ki, and Kd are the proportional, integral, and derivative gains, respectively.

4.2. Hybrid fuzzy-PD controller

To enhance robustness under variable operating conditions, a hybrid fuzzy–PD controller augmented with an integral action is implemented. The proposed control scheme combines the fast dynamic response of a fuzzy PD controller with an integral term to improve system stability, reduce overshoot, and eliminate steady-state errors. This hybrid structure is particularly well suited for motor drives operating under variable energy sources, such as solar-powered systems [22]. The controller inputs are defined as:

- Error: E=Ke·e(t)
- Derivative of error: $DE = Kde \cdot de(t)/dt$

the control output is expressed as:

$$ufuzzy = Kf \cdot uPD + Ki\_fz \cdot \int e(t)\, dt \quad (19)$$

Triangular membership functions are employed for both inputs, with three linguistic terms (negative, zero, positive) covering the expected ranges of the error and its derivative. The fuzzy inference system is constructed using a 3×3 rule base, resulting in a total of nine fuzzy rules.

Defuzzification is performed by combining the fuzzy PD output with the integral contribution through a weighted summation, yielding the final control signal applied to the motor drive [23]-[25]. To provide a clearer understanding of the control strategy, the operational procedure of the proposed hybrid fuzzy-PD controller is outlined in Algorithm 1.

Figure 6 illustrates the simulation of the solar-powered cable-driven robotic system. The control block represents the implemented PID, hybrid fuzzy-PD controllers, while the motor is simulated numerically in MATLAB.

Algorithm 1. Simplified hybrid fuzzy-PD control algorithm

```
Initialize:
 integral_e ← 0
 prev_e ← 0
Loop (for each sampling time t):
 Measure actual motor speed ω
 Read reference speed ω_ref
 Error computation
 e ← ω_ref − ω
 de ← (e − prev_e) / dt
 Input scaling
 E ← Ke × e
 DE ← Kde × de
Fuzzy PD inference
 u_PD ← FuzzyInference(E, DE)
 Integral update
 integral_e ← integral_e + e × dt
Hybrid control law
 u_fuzzy ← Kf × u_PD + Ki_fz × integral_e
Apply control signal
Apply u_fuzzy to motor drive
Update previous error
 prev_e ← e
End Loop
```

Figure 6. Simulation of the solar-powered cable-driven robotic system implemented in MATLAB

5. RESULTS AND DISCUSSION

The speed response comparison of four motors under PID and fuzzy control is shown in Figure 7. This figure illustrates the behaviour of each motor during the simulation. The curves demonstrate that both controllers achieve the target speed effectively. Furthermore, Table 1 presents the speed regulation performance metrics for all four motors.

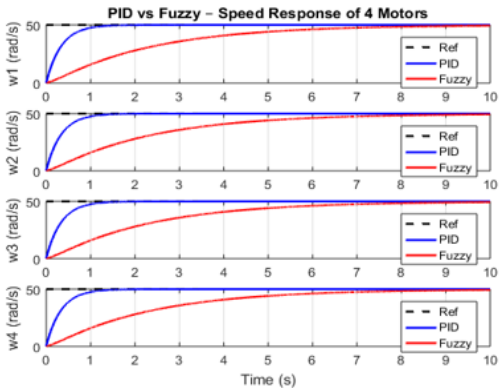

Figure 7. Comparison speed response of 4 motors PID/FUZZY control

Table 1. Speed regulation performance

Motor	RMS_PID	RMS_Fuzzy	Overshoot_PID	Overshoot_Fuzzy	Settling_PID	Settling_Fuzzy
1-4	6.42-6.50	5.10-5.20 ★	9-11	5-6 ★	1.28-1.35	1.08-1.12 ★

The position response comparison of four motors under PID and fuzzy control is presented in Figure 8. This figure highlights the dynamic behaviour of the motor positions during simulation. The results indicate that both control strategies manage to achieve stable position tracking. As shown in Table 2, these results indicate that the fuzzy controller offers better position tracking performance.

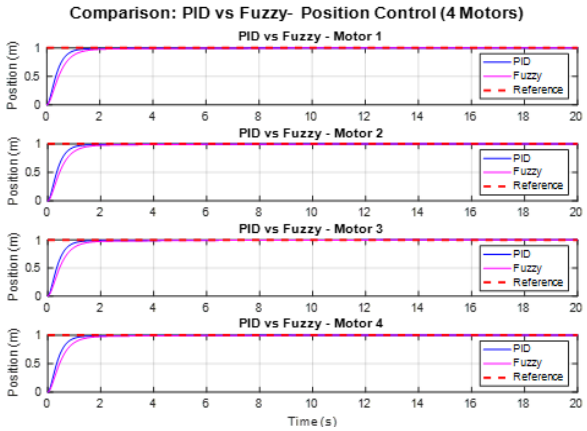

Figure 8. Comparison position response of 4 motors PID/fuzzy control

Table 2. Position tracking performance

Motor	RMS_PID	RMS_Fuzzy	Overshoot_PID	Overshoot_Fuzzy	Settling_PID	Settling_Fuzzy
1–4	0.11	0.09 ★	0.00	0.00	1.44	1.20 ★

The influence of solar power on the trajectory tracking performance of the cable-driven robot is illustrated in Figure 9. This figure analyses the dynamic behaviour of the system when powered by renewable energy. The results confirm that the robot maintains high precision in tracking the reference trajectory effectively.

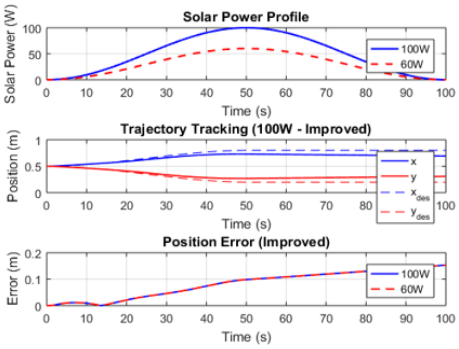

Figure 9. Solar power influence on trajectory tracking performance of the cable-driven robot

Enhanced trajectory tracking and motor responses using the fuzzy–PID controller are in Figure 10. This figure clearly highlights the superiority of the hybrid approach in optimizing the system performance. The presented outcomes prove that the proposed controller achieves faster convergence and smoother tracking transitions.

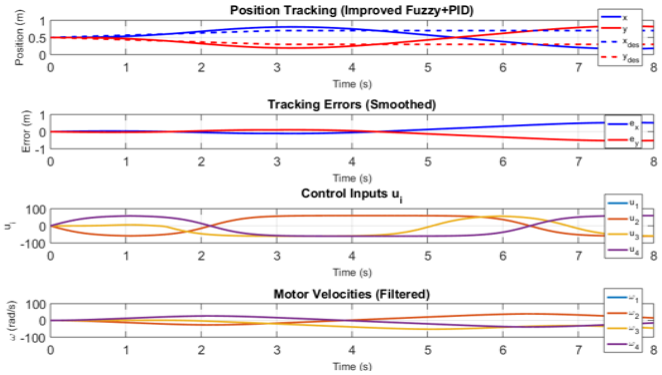

Figure 10. Enhanced tracking and motor response (fuzzy–PID)

6. INTEPRETATION OF RESULTS

The comparison between the conventional PID controller and the proposed fuzzy logic–based controller across the four motors reveals highly consistent and symmetrical behaviour, confirming proper load distribution and structural balance of the system. For all actuators, the fuzzy controller demonstrates superior speed regulation performance. Specifically, the RMS speed error is reduced from 6.42–6.50 to 5.10–5.20, corresponding to an average improvement of approximately 20%. In addition, overshoot decreases significantly from 9–11% to 5–6%, representing nearly a 45% reduction in peak deviation. The settling time is also shortened from 1.28–1.35 s to 1.08–1.12 s, indicating faster transient stabilization.

A similar enhancement is observed in the position response. The fuzzy-based controller lowers the RMS position error from 0.11 to 0.09 while reducing the settling time from 1.44 s to 1.20 s. In both control approaches, overshoot remains zero in position tracking, confirming stable trajectory convergence. These improvements highlight the ability of the fuzzy controller to better adapt to dynamic variations compared to the fixed-parameter structure of the classical PID controller.

Under photovoltaic power constraints (Pmax = 100 W, Figure 9), the system maintains stable trajectory tracking performance. The final position error reaches 0.1968 m, with an RMS tracking error of 0.2125 m. Although a maximum transient deviation of 0.2749 m occurs at t = 47.40 s, it remains temporary and does not compromise overall system stability. This behaviour demonstrates that the control strategy is capable of operating effectively under energy-limited conditions, which is essential for solar-powered robotic platforms.

Further performance enhancement is achieved using the hybrid fuzzy–PD controller (Figure 10). Despite exhibiting a moderate transient overshoot of 0.750 m, the controller maintains a bounded RMS tracking error of 0.375 m. The symmetric responses observed along both the x- and y-axes confirm the robustness of the proposed approach in the presence of cable nonlinearities and variations in solar power input.

Overall, the results clearly demonstrate that fuzzy logic–based control strategies, particularly the hybrid fuzzy–PD scheme, provide improved accuracy, faster transient response, and enhanced robustness compared to classical PID control. These characteristics make them especially suitable for solar-powered cable-driven robotic systems operating under nonlinear and energy-constrained conditions.

7. CONCLUSION

This study presented a control-oriented analysis of a solar-powered cable-driven robot, addressing the challenges arising from cable-induced nonlinearities and time-varying energy availability. Simulation results demonstrated that intelligent control strategies, particularly the hybrid fuzzy-based approach, improve motion stability and trajectory tracking performance compared to conventional PID control under fluctuating solar power conditions. These results emphasize the relevance of incorporating energy-aware control schemes in robotic systems powered by renewable and inherently variable energy sources.

While the proposed approach was evaluated using a simplified model and numerical simulations, the findings provide a meaningful foundation for future experimental validation. Ongoing work will focus on implementing the proposed control strategy on a physical robotic platform and exploring adaptive and real-time control methods to better handle environmental uncertainties. From an application perspective, the proposed approach shows promise for renewable-energy-powered tasks such as facade cleaning, greenhouse maintenance, and similar automated operations, where both stability and energy efficiency are critical. Future research will also address energy management optimization and long-term system reliability under prolonged solar variability.

ACKNOWLEDGMENTS

The authors would like to thank the hosting institution and laboratory for providing the necessary facilities to conduct this research. The authors also sincerely appreciate the constructive comments of the anonymous reviewers, which significantly improved the quality of this manuscript.

FUNDING INFORMATION

This research received no external funding.

AUTHOR CONTRIBUTIONS STATEMENT

This journal uses the Contributor Roles Taxonomy (CRediT) to recognize individual author contributions, reduce authorship disputes, and facilitate collaboration.

Name of Author	C	M	So	Va	Fo	I	R	D	O	E	Vi	Su	P	Fu
Kendouli Fairouz	✓	✓	✓		✓				✓					
Hemama Aboud				✓		✓		✓		✓				
Abed Khoudir										✓		✓	✓	

C : **C**onceptualization
M : **M**ethodology
So : **So**ftware
Va : **Va**lidation
Fo : **Fo**rmal analysis
I : **I**nvestigation
R : **R**esources
D : **D**ata Curation
O : Writing - **O**riginal Draft
E : Writing - Review & **E**diting
Vi : **Vi**sualization
Su : **Su**pervision
P : **P**roject administration
Fu : **Fu**nding acquisition

CONFLICT OF INTEREST STATEMENT

The authors declare no conflict of interest.

DATA AVAILABILITY

The data supporting the findings of this study are available from the corresponding author upon reasonable request.

REFERENCES

[1] R. Wang, J. Li, and Y. Li, "A review on design, modeling and control technology of cable-driven parallel robots," *Robotics*, vol. 14, no. 9, p. 116, Aug. 2025, doi: 10.3390/robotics14090116.

[2] X. Jin, H. Zhang, L. Wang, and Q. Li, "Review on control strategies for cable-driven parallel robots with model uncertainties," *Chinese Journal of Mechanical Engineering*, vol. 37, no. 1, p. 156, Dec. 2024, doi: 10.1186/s10033-024-01149-8.

[3] N. G. E006C Sayed, A. M. Yousef, G. El-Saady, M. D. Alanazi, H. A. Ziedan, and M. Abdelsattar, "Electrical grid linked to PV/wind system based fuzzy controller and PID controller tuned by PSO for improving LVRT," *Scientific Reports*, vol. 15, no. 1, p. 7698, Mar. 2025, doi: 10.1038/s41598-025-87208-z.

[4] Y. H. Alwan, A. A. Oglah, and M. S. Croock, "Optimized robust fuzzy PID controller for suspended cable-driven parallel robots via dragonfly algorithm," *Mechanics*, vol. 31, no. 6, pp. 567-577, Dec. 2025, doi: 10.5755/j02.mech.41438.

[5] M. T. Vu, K. H. Hsia, F. F. M. El-Sousy, T. Rojsiraphisal, R. Rahmani, and S. Mobayen, "Adaptive fuzzy control of a cable-driven parallel robot," *Mathematics*, vol. 10, no. 20, p. 3826, Oct. 2022, doi: 10.3390/math10203826.

[6] Y. H. Alwan, A. A. Oglah, and M. S. Croock, "Optimized adaptive fuzzy synergetic controller for suspended cable-driven parallel robots," *Automation*, vol. 6, no. 2, p. 15, Apr. 2025, doi: 10.3390/automation6020015.

[7] S. Zare, M. R. H. Yazdi, M. T. Masouleh, D. Zhang, S. Ajami, and A. A. Ardekani, "Experimental study on the control of a suspended cable-driven parallel robot for object tracking purpose," *Robotica*, vol. 40, no. 11, pp. 3863-3877, Nov. 2022, doi: 10.1017/S0263574722000649.

[8] P. Fang *et al.*, "Design and implementation of a 3-DOF modular high-rise façade-cleaning robot with an XYZ motion module," *Machines*, vol. 13, no. 4, p. 294, Apr. 2025, doi: 10.3390/machines13040294.

[9] J. Wang *et al.*, "Design and self-calibration method of a rope-driven cleaning robot for complex glass curtain walls," *Actuators*, vol. 13, no. 7, p. 272, Jul. 2024, doi: 10.3390/act13070272.

[10] F. Hou, C. Liu, H. Jiang, Z. Tang, P. Fang, and S. Wang, "Structural design and control strategy of a cable-driven robot under high-altitude facade conditions with large span and multiple constraints," *Industrial Robot*, vol. 51, no. 6, pp. 947-959, Dec. 2024, doi: 10.1108/IR-03-2024-0097.

[11] A. Antonov, "Parallel-serial robotic manipulators: a review of architectures, applications, and methods of design and analysis," *Machines*, vol. 12, no. 11, p. 811, Nov. 2024, doi: 10.3390/machines12110811.

[12] B. Hu, Z. Xu, R. Wang, M. Feng, and N. Ye, "Inverse kinematics of 2 (3RPS) and 2 (3SPR) serial-parallel manipulators," *Chinese Journal of Mechanical Engineering*, vol. 38, no. 1, p. 45, Apr. 2025, doi: 10.1186/s10033-025-01196-9.

[13] Z. Zhang, D. Zhu, and D. Li, "Conformal geometric algebra-based forward kinematics analysis method for the (2-SPR+RPS)+(3-SPR) serial-parallel hybrid mechanism," *Chinese Journal of Mechanical Engineering*, vol. 38, no. 1, p. 140, Aug. 2025, doi: 10.1186/s10033-025-01325-4.

[14] Z. Zhang, L. Yang, C. Sun, W. Shang, and J. Pan, "CafkNet: GNN-empowered forward kinematic modeling for cable-driven parallel robots." Nov. 25, 2024. [Online]. Available: http://arxiv.org/abs/2402.18420

[15] R. Wang, Y. Xie, X. Chen, and Y. Li, "Kinematic and dynamic modeling and workspace analysis of a suspended cable-driven parallel robot for schönflies motions," *Machines*, vol. 10, no. 6, p. 451, Jun. 2022, doi: 10.3390/machines10060451.

[16] R. Bitriá and J. Palacín, "Optimal PID control of a brushed DC motor with an embedded low-cost magnetic quadrature encoder for improved step overshoot and undershoot responses in a mobile robot application," *Sensors*, vol. 22, no. 20, p. 7817, Oct. 2022, doi: 10.3390/s22207817.

[17] K. Moussa, M. Thieffry, F. Claveau, P. Chevrel, and S. Caro, "Dynamic models for simulation of cable-driven parallel robots with elasticity and sagging," *Mechanism and Machine Theory*, vol. 209, p. 105972, Jul. 2025, doi: 10.1016/j.mechmachtheory.2025.105972.

[18] A. Salem, M. Abdel-Ghany, and ş. O. Ibrahim, "Performance enhancement of dc-motor based on multi different control techniques," *International Journal of Engineering and Applied Sciences-October 6 University*, vol. 2, no. 2, pp. 38-44, Jul. 2025, doi: 10.21608/ijeasou.2025.387627.1052.

[19] A. Senturk and R. Eke, "A new method to simulate photovoltaic performance of crystalline silicon photovoltaic modules based on datasheet values," *Renewable Energy*, vol. 103, pp. 58-69, Apr. 2017, doi: 10.1016/j.renene.2016.11.025.

[20] T. N. Olayiwola, S. H. Hyun, and S. J. Choi, "Photovoltaic modeling: a comprehensive analysis of the i–v characteristic curve," *Sustainability*, vol. 16, no. 1, p. 432, Jan. 2024, doi: 10.3390/su16010432.

[21] V. Rajs, N. L. Raševic, M. Z. Bodic, M. M. Zukovic, and K. B. Babkovic, "PID controller design for motor speed regulation with linear and non-linear load," *IFAC-PapersOnLine*, vol. 55, no. 4, pp. 225-229, 2022, doi: 10.1016/j.ifacol.2022.06.037.

[22] J. M. R. Chintu, R. K. Sahu, and S. Panda, "Adaptive differential evolution tuned hybrid fuzzy PD-PI controller for automatic generation control of power systems," *International Journal of Ambient Energy*, vol. 43, no. 1, pp. 515-530, Dec. 2022, doi: 10.1080/01430750.2019.1653986.

[23] N. T. Pham, T. D. Le, and P. D. Nguyen, "Direct torque control of induction motor using a novel higher-order sliding mode control," *International Journal of Intelligent Engineering and Systems*, vol. 18, no. 7, pp. 131–143, Aug. 2025, doi: 10.22266/ijies2025.0831.10.

[24] J. R. García-Martínez, E. E. Cruz-Miguel, R. V. Carrillo-Serrano, F. Mendoza-Mondragón, M. Toledano-Ayala, and J. Rodríguez-Reséndiz, "A PID-type fuzzy logic controller-based approach for motion control applications," *Sensors*, vol. 20, no. 18, pp. 1–19, Sep. 2020, doi: 10.3390/s20185323.

[25] C. T. Chao, N. Sutarna, J. S. Chiou, and C. J. Wang, "Equivalence between fuzzy PID controllers and conventional PID controllers," *Applied Sciences*, vol. 7, no. 6, p. 513, Jun. 2017, doi: 10.3390/app7060513.

BIOGRAPHIES OF AUTHORS

Kendouli Fairouz associate professor in the transport engineering department, Mentouri Brothers University, Constantine Algeria. Head of research team in Electrical Engineering Laboratory of Constantine (LGEC), His professional research in: intelligent control, field-oriented control and direct power control for machines drives, renewable and green energies, modeling and simulation of wind and solar energy conversion system. She can be contacted at email: kendouli.fairouz@umc.edu.dz.

Hemama Aboud was born in Oum El Bouaghi, Algeria, and graduated with a degree in Mechanical Engineering from the Faculty of Science and Technology, University of LarbiBen M'hidi, Algeria, in 2000. She earned her master's degree in robotics and intelligent systems from LarbiBen M'hidi University, Oum El Bouaghi, Algeria, in 2009. In 2014, she was appointed as an assistant professor in the Department of Transport Engineering at the Faculty of Science and Technology, Frères Mentouri Constantine 1 University. Her research interests include robotics. She can be contacted at email: aboud.hemama@umc.edu.dz.

Khoudir Abed professor in the electrical engineering department, Mentouri Brothers University, Constantine Algeria. Head of research team in Electrical Engineering Laboratory of Constantine (LGEC), His professional research in: intelligent control, fuzzy logic and field-oriented control and direct torque control for AC machines drives. Renewable and green energies. He can be contacted at email: abed.khoudir@umc.edu.dz.